DIAGNOSTIC NEURORADIOLOGY

Developmental venous anomalies: appearance on whole-brain CT digital subtraction angiography and CT perfusion

**Eric H. Hanson · Cayce J. Roach · Erik N. Ringdahl · Brad L. Wynn ·
Sean M. DeChancie · Nathan D. Mann · Alan S. Diamond · William W. Orrison Jr.**

Abstract

Introduction Developmental venous anomalies (DVA) consist of dilated intramedullary veins that converge into a large collecting vein. The appearance of these anomalies was evaluated on whole-brain computed tomography (CT) digital subtraction angiography (DSA) and CT perfusion (CTP) studies.

Methods CT data sets of ten anonymized patients were retrospectively analyzed. Five patients had evidence of DVA and five age- and sex-matched controls were without known neurovascular abnormalities. CT angiograms, CT arterial-venous views, 4-D CT DSA and CTP maps were acquired on a dynamic volume imaging protocol on a 320-detector row CT scanner. Whole-brain CTP parameters were evaluated for cerebral blood flow (CBF), cerebral blood volume (CBV), time to peak (TTP), mean transit time (MTT), and delay. DSA was utilized to visualize DVA anatomy. Radiation dose was recorded from the scanner console.

Results Increased CTP values were present in the DVA relative to the unaffected contralateral hemisphere of 48%, 32%, and 26%; and for the control group with matched hemispheric comparisons of 2%, −10%, and 9% for CBF, CBV, and MTT, respectively. Average effective radiation dose was 4.4 mSv.

Conclusion Whole-brain DSA and CTP imaging can demonstrate a characteristic appearance of altered DVA

E. H. Hanson · C. J. Roach
Advanced Medical Imaging and Genetics (Amigenics),
5495 South Rainbow Boulevard, Suite 201,
Las Vegas, NV 89118, USA

E. H. Hanson · S. M. DeChancie · N. D. Mann · W. W. Orrison Jr.
Touro University Nevada College of Osteopathic Medicine,
874 American Pacific Drive,
Henderson, NV 89014, USA

E. H. Hanson · W. W. Orrison Jr.
Department of Health Physics and Diagnostic Sciences,
University of Nevada Las Vegas,
4505 Maryland Parkway, Box 453037, Las Vegas, NV 89154,
USA

C. J. Roach
School of Life Sciences, University of Nevada Las Vegas,
4505 Maryland Parkway,
Las Vegas, NV 89154-4004, USA

E. N. Ringdahl
Department of Psychology, University of Nevada Las Vegas,
4505 Maryland Parkway,
Las Vegas, NV 89154-3034, USA

B. L. Wynn
Family Medicine Spokane,
104 West 5th, Suite 200W,
Spokane, WA 99204, USA

A. S. Diamond · W. W. Orrison Jr.
CHW Nevada Imaging Company, Nevada Imaging Centers,
Spring Valley,
5495 South Rainbow Boulevard, Suite 101,
Las Vegas, NV 89118, USA

W. W. Orrison Jr.
Department of Medical Education,
University of Nevada School of Medicine,
1664 North Virginia Street,
Reno, NV 89557, USA

E. H. Hanson (✉)
Amigenics, Inc,
5495 South Rainbow Boulevard, Suite 201,
Las Vegas, NV 89118, USA
e-mail: eric.hanson@amigenics.com

hemodynamic parameters and capture the anomalies in superior cortices of the cerebrum and the cerebellum. Future research may identify the rare subsets of patients at increased risk of adverse outcomes secondary to the altered hemodynamics to facilitate tailored imaging surveillance and application of appropriate preventive therapeutic measures.

Introduction

Developmental venous anomalies (DVA) represent a normal variant that may be associated with other cerebral vascular malformations. DVA have been previously referred to as venous angiomas, venous malformations, and medullary venous malformations [1]. DVA can be located throughout the brain and have been described as being juxtacortical, subcortical, or deep. Deep DVA are further subdivided by supratentorial and infratentorial location [2]. Macroscopically, DVA have been described as dilated thin-walled medullary vessels that drain white and gray matter radially and centripetally into a larger caliber collecting or draining vein that opens into superficial subcortical or deep pial veins [3, 4].

DVA represent nearly 60% of all cerebral vascular variations (often classified as malformations) at autopsy [5]. In a craniospinal magnetic resonance imaging (MRI) survey of 8,200 patients, DVA were present in 50, suggesting a point prevalence of 0.6% [6]. A postmortem study of 4,069 cases reported that DVA were present in 2.5% [7]. DVA are known to be associated with vascular malformations including arteriovenous malformation (AVM), cavernous malformations (CM), and capillary telangiectasias [8, 9]. Up to a third of patients with DVA may have a second cerebrovascular abnormality, such as CM [9]. Isolated DVA are considered to be congenital in nature and generally follow a benign natural history. However, symptomatic DVA have been increasingly clinically identified [10] and neurologic symptoms, such as headaches, seizures, paresthesias, motor deficits, trigeminal neuralgia, and extrapyramidal disorder have been reported [11].

DVA have been identified on computed tomography (CT), magnetic resonance imaging (MRI), single photon emission computed tomography (SPECT), conventional angiography, and digital subtraction angiography (DSA) and may display several characteristic imaging features on each of these modalities. On contrast-enhanced CT, the linear or curvilinear features of the venous collection system are frequently present. On noncontrast MR, DVA can appear as tubular signal voids on T1- and T2-weighted sequences [8] and variable degrees of T1 and T2 prolongation may be seen in adjacent parenchyma [12]. On contrast-enhanced MRI, the draining veins enhance to provide improved visualization of DVA structure. On diffusion-weighted imaging, DVA that are thrombosed or infarcted may appear as a region of restricted diffusion with a bright signal intensity [13]. Perfusion MR studies have demonstrated increased perfusion values [12, 14]. However, CT perfusion (CTP) parameters of DVA have only been recently described [15]. This may be secondary to limitations of whole-brain coverage in previous technology that did not allow full visualization in the peripheral or superior cerebral cortices.

Recent advances in the understanding of flow-related pathomechanisms of DVA include an increased risk of symptomatology secondary to their in- and outflow hemodynamics [10]. Hemodynamic changes that can be detected by imaging may be caused by collecting vein outflow obstruction, progressive thickening of vein walls, and structural organization in the venous convergence zone [16]. DVA with a vascular malformation, arteriovenous shunting, and an arterialized DVA have been described as early appearing vessels with a capillary blush in the arterial phase and early venous filling on angiography [17]. Such DVA variations may increase the clinical risk of these lesions and may therefore require more frequent assessments.

In this study, five cases of DVA, as well as age- and sex-matched controls, were retrospectively identified on whole-brain CT DSA and whole-brain CTP to evaluate if the increased anatomical coverage on whole-brain CTP and the collection of relative CTP parameters could provide incremental diagnostic information for DVA identification and diagnosis.

Materials and methods

This study was a retrospective and anonymized study of CT scans obtained for clinical purposes. This study was performed with Institutional Review Board exemption approval and was Health Information Portability and Accountability Act compliant.

Demographic data Cases and controls were identified retrospectively in a consecutive manner from CTP examinations completed without complications or technical failures between April and December 2008. Clinical characteristics, CT indications, and DVA descriptions are listed in Table 1. All scans were considered diagnostic with excellent definition of DVA vascular structures on CT DSA and hemodynamic information on CTP.

Table 1 Age- and sex-matched controls (ranging from 2 years older to 7 years younger) were selected if there was no evidence of brain vascular abnormalities on CTP ordered for clinical indications listed below.

	Age (year); sex	Clinical CT indication	DVA location and description	Figures
Case 1	50; female	Right facial numbness	Juxtacortical left frontal lobe DVA with a superficial collecting vein	Fig. 5 Fig. 1
Control 1	49; female	Prior increased T2 signal in pons on MRI	No abnormalities	Fig. 1
Case 2	63; male	Carotid bruit preoperative assessment	Juxtacortical left frontal lobe DVA with a superficial collecting vein	Fig. 3
Control 2	62; male	Headaches	Mild cerebral atrophy consistent with age	
Case 3	64; male	Prior abnormal CT scan	Subcortical right cerebellar hemisphere DVA with 4 dilated intramedullary veins that converge into a superficial draining vein near lateral right transverse venous sinus	Fig. 4
Control 3	66; male	Rule out vertebral artery stenosis	Mild cerebral atrophy consistent with age. Vertebral artery calcification not causing stenosis	
Case 4	28; male	Evaluation of a possible AVM identified on MRI	Subcortical left parietal region DVA and deep collecting vein	
Control 4	21; male	History of carbon monoxide exposure	No abnormalities	
Case 5	29; female	History of carbon monoxide exposure	Left juxtacortical frontal lobe DVA with a superficial collecting vein	
Control 5	29; female	History of carbon monoxide exposure	No abnormalities	

Controls were analyzed to provide baseline values and comparison of case hemispheric CTP values

The 320-detector row dynamic volume CT technique Scans were performed on a 320-detector row configuration CT scanner (Aquilion ONE, Toshiba Medical Systems, Nasu, Japan). CT imaging protocol, hardware, software, and perfusion parameters are listed in Table 2. The CT protocol provided CT angiography (CTA), CT arterial-venous view (CTA-V), four-dimensional (4D) CT DSA, and whole-brain CTP. Radiation doses were estimated using the CT console dose length product (DLP) and converted to effective dose as milliSieverts (mSv) using the conversion factor for CT of the head (DLP×0.0023) according to the European Guidelines for Multislice CT (Table 2) [18].

Image analysis All clinical data (CTA, CTA-V, 4D DSA, and CTP) were retrospectively interpreted by two neuroradiologists (A.D. with 17 years and W.O. with 26 years of

Table 2 The 320-detector row CT hardware, software, protocol and CTP parameters utilized in this study.

CT configuration	320×0.5 mm detector row
Contrast amount	50-70 ml by automated antecubital venous injection
Contrast infusion rate	4-6 ml/s
Reconstructed section thickness and section interval	0.5 mm with 0.5 mm reconstruction interval
Section collimation	0.5 mm
CT matrix	512×512
Kilovolts (kVp)	80 kVp
Milliamp (mA)	100 mA for 21 individual data sets in cases 1-4. Initial 300 mA then 100 mA series for 19 individual data sets in case 5
Size of detector array; field of view	160 mm
Software and version	Vitrea *fX* version 2.0.2
Singular value decomposition (SVD) cutoff threshold	5%
Perfusion algorithm utilized	SVD+
Vascular pixel elimination	On
Dose length product to milliSieverts (mSv)	4.3 mSv for cases 1-4 and 4.4 mSv for case 5
Arterial input function selection location	Middle cerebral artery M1 segment
Venous input function location	Superior sagittal sinus
Automatic or manual arterial input and venous input function selections	Manual contralateral unaffected hemisphere for case 1. Automatic arterial input function and venous input function selection for cases 2-5
Region of interest (ROI) dimensions	8 mm diameter×0.5 mm depth

neuroradiology experience). Each volume acquisition was assessed in the cine mode for the presence of motion. No volumes were removed because of motion, metal, or artifacts near the DVA. Automatic arterial input function selections were moved to the contralateral side of the abnormality if the arterial input function was automatically placed on the affected side by the software (case 1). Venous inputs were manually moved to the superior sagittal sinus if the venous input was automatically positioned near the DVA (case 3). DVA were assessed by lobar or cerebellar location and juxtacortical or subcortical depth following the descriptions of Lee et al. [19]. Juxtacortical was defined as within the gray matter or within the gray-white matter junction and subcortical was defined as below the juxtacortical region but not adjacent to the ventricular wall. The draining or collecting vein to which the caput medusae were joined was classified as either deep toward the ventricle and central aspects of the brain or superficial toward the brain surface [19]. No associated CM or other vascular anomalies were identified.

Analyzed CTP values included regional cerebral blood volume (CBV), regional cerebral blood flow (CBF), mean transit time (MTT), time to peak (TTP), and delay. Delay is a CTP parameter unique to the Vitrea *fX* software and is derived computationally from the first identified contrast in the time-intensity graph and is independent of the contrast injection rate. Delay is measured as the time in seconds for the computed residue function to reach maximum. To collect quantitative CTP values, a template of three regions of interest (ROI) circles measuring 8 mm in diameter and 0.5 mm thickness were placed 3 mm apart in a triangular pattern within the DVA at a single axial slice level. Three ROIs were also placed in the contralateral or unaffected hemisphere for intraindividual comparison. This identical bilateral hemisphere ROI template was then placed in the same location for each control (case 1 and control 1 in Fig. 1). Absolute values were defined by the ROI CTP values. Relative values were the percent change in CTP values between each ROI from one hemisphere and the contralateral hemisphere. Axial perfusion images for the five cases were analyzed for absolute and relative values at the DVA level and compared with the unaffected hemisphere. Hemispheric orientation of the controls was matched to the affected (i.e., hemisphere with DVA) and unaffected hemispheric location of each case.

Statistical analysis Analyses of the ROI absolute and relative values by hemisphere for cases and controls included maximum, minimum, first quartile (Q1), third quartile (Q3), median, and outlier CTP values (i.e., value greater than ±1.5 standard deviation from Q1 and Q3). Box and whisker diagrams (box plots) were generated to depict outlier values for absolute and relative CTP values. Grubb's

test analysis confirmed outliers for box plot results as described by Barnett [20]. Independent *t* tests assuming equal variances compared the absolute and relative values. Absolute values for cases and controls are shown in Fig. 2. Relative hemispheric comparisons of the three ROIs for each case and control group are described in Table 3. Relative case values were calculated for cases by determining the percentage change between three ROI CTP values of the affected hemisphere and contralateral or unaffected hemisphere. Relative control values were calculated for the five age- and sex-matched controls by maintaining hemispheric alignment with the DVA cases and then comparing the affected to the unaffected hemisphere values.

Results

Absolute and relative CBV and CBF values were higher for the five cases in the affected hemisphere compared to the unaffected hemisphere indicating increased blood volume and flow within and surrounding the DVA. Relative values for DVA cases (affected versus unaffected hemisphere) and relative values for controls with hemispheres of brain compared in same orientation as the cases were compared as groups by perfusion parameter using independent two sample *t* tests. Statistically significant increases for CBV of 48.28% ($p < 0.001$; 95% CI=29.45-62.75%) and for CBF of 31.95%   ($p < 0.001$; 95% CI=25.66-57.42%) were present for the affected hemispheres of the five cases versus their unaffected hemisphere (Table 3). Three outlier values for relative CBV and two outliers for CBF within the values were included in the analyses (Fig. 2a). Relative CBV, CBF, and MTT for the case affected hemispheres were 45.87%, 37.89%, and 11.11% higher versus the control affected hemispheres, respectively (Table 3).

Relative MTT values for the five cases were significantly increased on the affected side (26.18%, $p=0.004$), with the exception of a single ROI relative value difference of ROI 2 in case 2 (3.3 vs. 3.1; 6.06%) higher on unaffected side. However, the higher percentage difference in case relative MTT of 26.18% (case-affected MTT versus case-unaffected MTT values) versus the relative affected case-to-control MTT of 11.11% (Table 3) was analyzed further to determine the source of the spread in these percentages by evaluating the absolute MTT values (Fig. 2). The difference in the case affected-to-unaffected absolute MTT values were statistically significant ($p=0.001$), while the difference for absolute MTT values for the case-to-control affected hemispheres was not statistically significant ($p=0.674$). Additionally, a comparison of case-to-control unaffected MTT values had marginal statistical significance ($p=0.058$). Median values for the case unaffected hemispheres was 3.70 s and the median for control
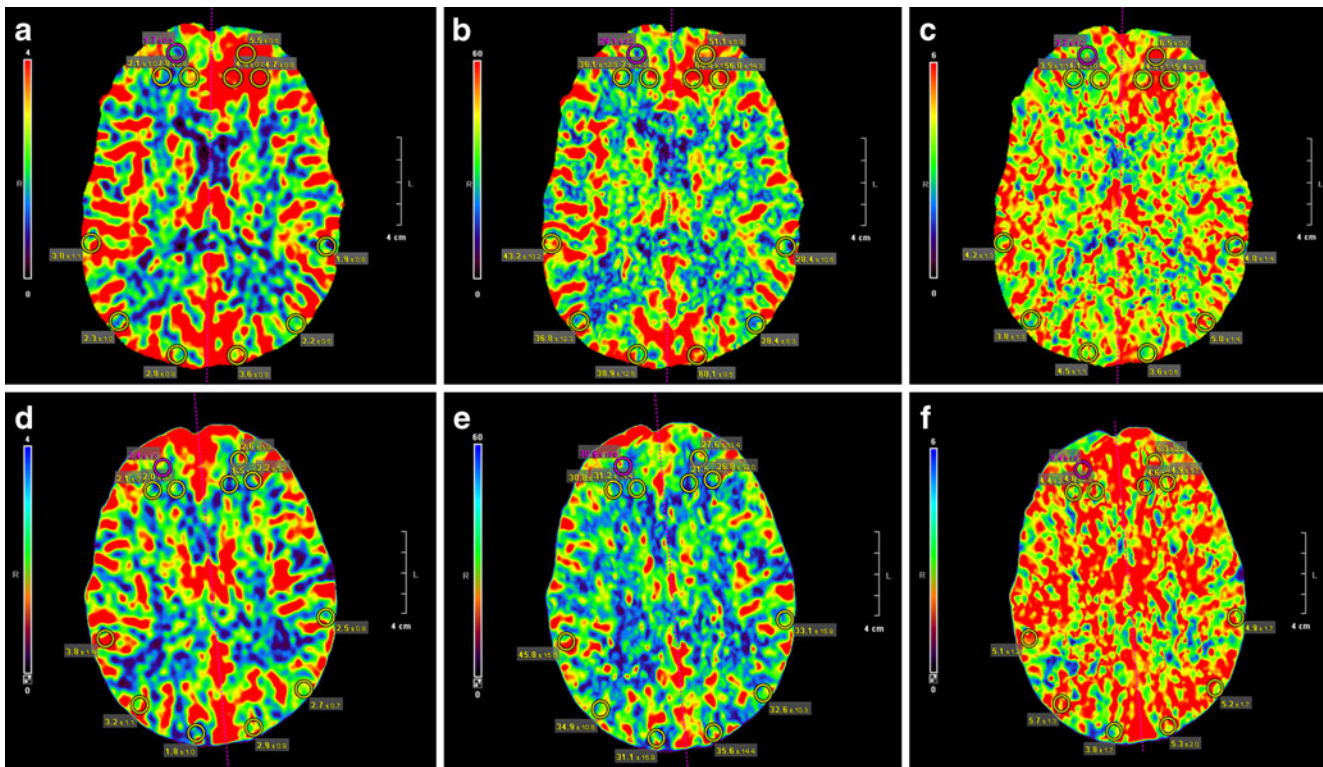
Fig. 1 Three ROIs measuring 8 mm in diameter and 0.5 mm thickness were placed 3 mm apart in a triangular pattern within the affected hemisphere and mirrored in the unaffected hemisphere (case 1 in the *upper row*; **a**, **b**, **c**). An identical ROI template was used for each control (control 1 in *lower row* **d**, **e**, **f**) to facilitate comparisons of absolute values and relative CTP percentages for regional CBV (**a**, **d**), regional CBF (**b**, **e**), and MTT (**c**, **f**)

unaffected hemisphere was 4.60 s, a decrease of 0.90 s. Comparison of CBV, CBF, TTP, and delay for case-to-control unaffected absolute values revealed no statistically significant differences.
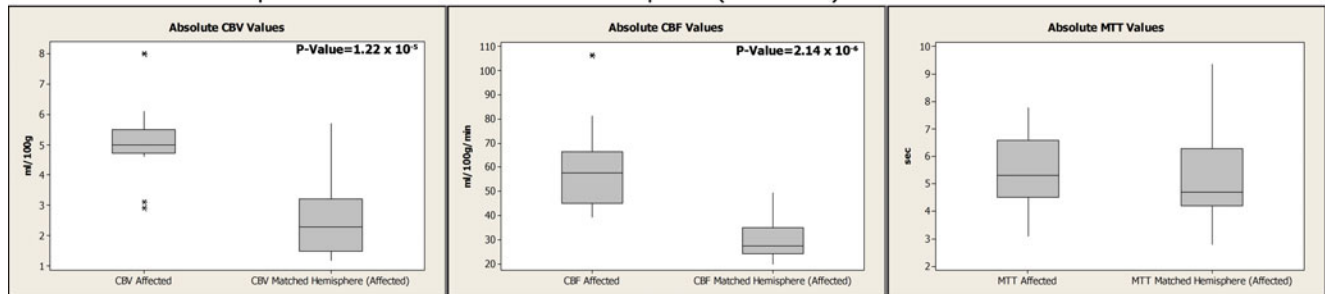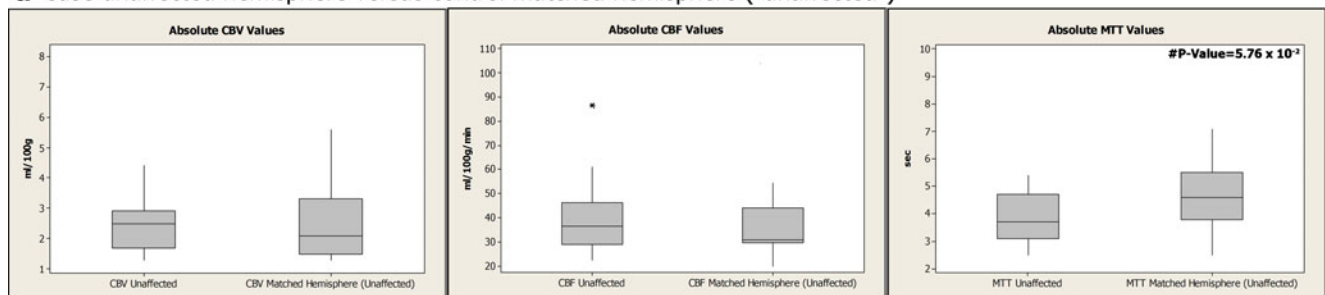
Average relative difference for TTP in the five cases was increased by 0.74% in the affected hemisphere versus the unaffected side; however, this was not statistically significant ($p=0.377$). Case 2 and case 5 had lower TTP values on the affected side versus contralateral side, suggesting a shorter arrival time for blood flow. Delay did not have a consistent pattern of increased or decreased CTP values in the DVA area.

Volumetric surface CTP maps in Fig. 3 demonstrate cortical-related changes from a left frontal juxtacortical caput medusa and superficial collecting vein that was significantly better defined on CTP as compared to the non-contrast MR obtained in this patient. Figure 4d is a CTA-V view of the venous phase for case 3 of a subcortical right cerebellar hemisphere DVA. Effective radiation dose for cases 1-4 was 4.3 mSv and 4.4 mSv for case 5.

Discussion

This study demonstrates that CTP may permit assessment of the hemodynamic alterations associated with DVA. For

each DVA in this study, absolute CBV and CBF values were significantly increased in the affected hemisphere as compared to the unaffected hemisphere. On MR perfusion, Camacho et al. [12] also identified increased CBF, CBV, and MTT in four uncomplicated DVA cases. The authors concluded that hemodynamic alterations were not associated with the presenting symptoms of the patients and that the alterations did not imply a more ominous future outcome for the DVA. The results of this study suggested that increased regional CBV and CBF on CTP may indicate the presence of a DVA on CTP of the brain and case 1 presented with facial numbness symptoms that may have been influenced by the presence of the DVA. Previous studies have identified decreased CBF values in the parenchyma near two large DVA on xenon-enhanced CT [21] and in one patient on brain perfusion SPECT that the authors believed was correlated with the SPECT abnormalities, DVA location, and an electroencephalograph focus [22]. However, differentiation of the intravascular hemodynamic changes and the surrounding parenchymal perfusion changes using the ROI approach in this study is limited due to the averaging of the CTP values within the ROI and future studies using a pixel-by-pixel evaluation of the DVA and the surrounding parenchyma could provide an answer.

Fig. 2 Box plots of absolute hemispheric values for three ROIs of CBV, CBF, and MTT for each case and control group included: **a** case-affected hemisphere versus case-unaffected hemisphere, **b** control-matched affected versus control-matched hemisphere unaffected, (**c**) case-affected versus control affected, and (**d**) case-unaffected versus control unaffected. Outlier values (*asterisk*) are depicted in the CTP parameter group as applicable. Significant *p* values are listed in the upper right corners and near statistical significance is preceded by a *pound sign*
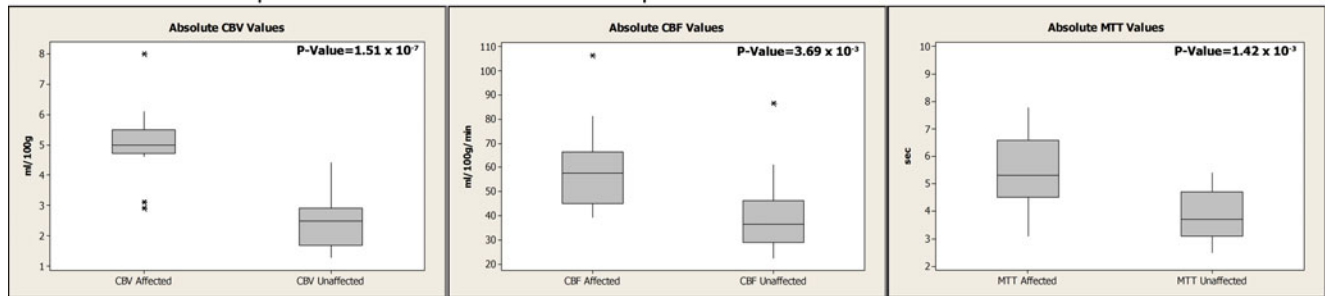
Although MTT was consistently elevated and suggestive of delayed or slow flow in this small group of five patients, further study is required to determine how the whole-brain hemodynamic (i.e., CBV and CBF) and temporal CTP values (i.e., MTT, TTP, and delay) within the DVA can be utilized to further delineate the hemodynamic parameters for a larger collection of DVA cases. Because MTT is an indicator of perfusion pressure, the higher MTT values in

the DVA indicated lower flow or perfusion and increased MTT values have previously been associated with DVA in four patients on MR perfusion [12]. The unaffected hemispheres of each case appeared to be influencing the relative percentage change in MTT values, but because of insignificant *p* values and the small sample size, evaluation of trends in MTT values in patients with a DVA over time will require further research.

Table 3 Analyses of the hemispheric comparisons of the aggregated ROI CTP values for case versus control group included: (1) case affected percent change versus case unaffected (relative case), (2) control affected percent change versus control unaffected (relative control); (3) case affected percent change versus control affected (relative affected); and (4) case unaffected percent change versus control unaffected (relative unaffected).

Hemispheric Comparison	CBV	CBF	MTT	TTP	Delay
Case affected versus Case unaffected	48.28%*	31.95%*	26.18%*	0.60%	−4.93%
P values	*4.45 x 10^{-6}	*1.05 x 10^{-5}	*4.27 x 10^{-3}	3.77 x 10^{-1}	5.64 x 10^{-1}
Control affected versus Control unaffected	2.17%	−9.59%	9.18%	−2.89%	2.27%
Case affected versus Control affected	45.87%	37.89%	11.11%	−5.71%	0.18%
Case unaffected versus Control unaffected	0.73%	−16.75%	22.46%	2.83%	−5.89%

P values are listed for case affected and unaffected hemisphere comparisons and statistical significance is indicated by an asterisk (*)

TTP results for DVA cases must be interpreted in the context of each individual patient. TTP was not indicative of DVA in this study. This was possibly due to the wide range of DVA types that can both increase and decrease the time for blood to get to a region. TTP is a temporal parameter that can be falsely prolonged depending on technical factors of the scanning process and by the size and shape of the arterial input function. Cases 1, 3, and 4 had higher relative TTPs in the affected hemisphere (range 1.99-6.45%) that suggested slower arrival of contrast to the DVA. This may be anticipated in slow flow venous structures with lower proportions of arterial influence on TTP values. For cases 2 and 5, rapid flow and lower relative TTP (−4.09% in case 5 to −7.43% in case 2) in the affected hemisphere could be interpreted as contribution from a possible arteriovenous shunting component but this could not be confirmed and no arterial abnormalities were noted on CT DSA for cases 2 and 5. Further DVA case analyses will be required to evaluate if TTP may serve as a stratifier for CTP pressures in DVA and a possible CTP

parameter that may, in combination with the CBV, CBF, and MTT results, help to delineate an individual's risk of future complications.

Flow-related complications of DVA that may lead to a symptomatic presentation include an increase of inflow because of an arteriovenous shunt, a decrease of outflow, or a remote shunt with increased venous pressure [10]. In our study, case 1 presented with symptoms that was possibly secondary to a DVA (Fig. 5). Pereira et al. suggested characteristics of an increased risk of symptomatic DVA presentation: large and complex DVA with changes on MRI suggesting venous congestion, acute or subacute ischemic changes, asymmetrical medullary zone appearance, and association with AVMs [10]. Mechanical compression of intracranial structures around the DVA produced symptoms in 20.3% (14 of 69 cases). Unexplained symptomatology occurred in 8.7% (six of 69 cases) while the remaining 71% (49 of 69 cases) of symptomatic DVA were attributed to flow-related pathomechanisms (19 with increased inflow, 26 with decreased outflow, and four with a shunt that
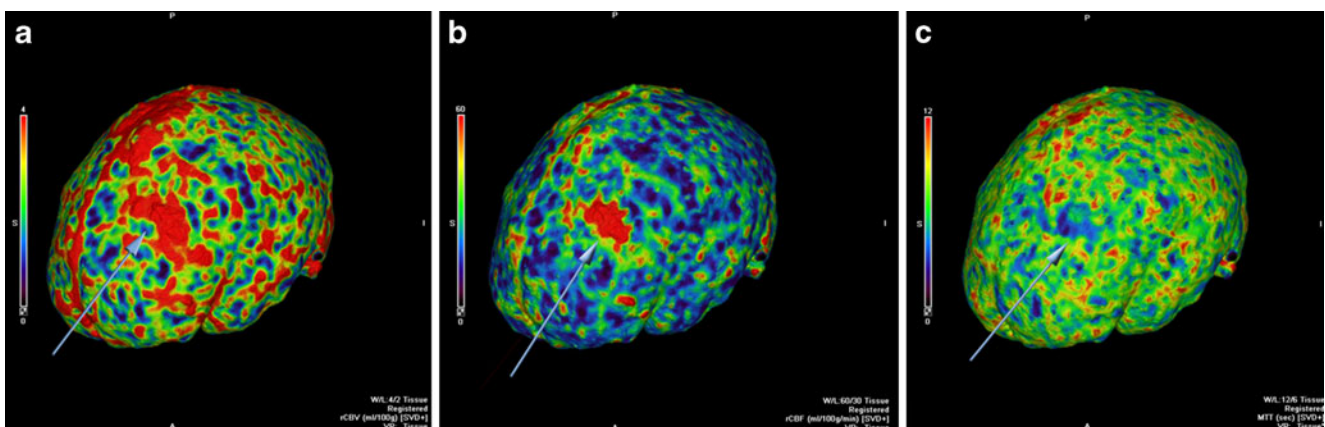
Fig. 3 Volumetric surface CT perfusion maps from case 2 of cortical changes (*arrows*) in regional CBV (**a**), regional CBF (**b**), and MTT (**c**) related to a left frontal juxtacortical DVA with a superficial collecting vein

Fig. 4 (**a**) A 64-year-old male with a subcortical right cerebellar hemisphere DVA on the right side (case 3) on axial DSA. Increased CTP values are present in the affected hemisphere (*arrows*) for regional CBV (**b**), regional CBF (**e**), and MTT (**f**) relative to the unaffected hemisphere. No significant differential TTP values were present (**c**). Orthogonally edited CTA-V view of the venous system, demonstrating the cerebellar hemisphere DVA on the right side with dilated intramedullary veins that converge into a collecting vein that enters the lateral aspect of the right transverse venous sinus is demonstrated (**d**)
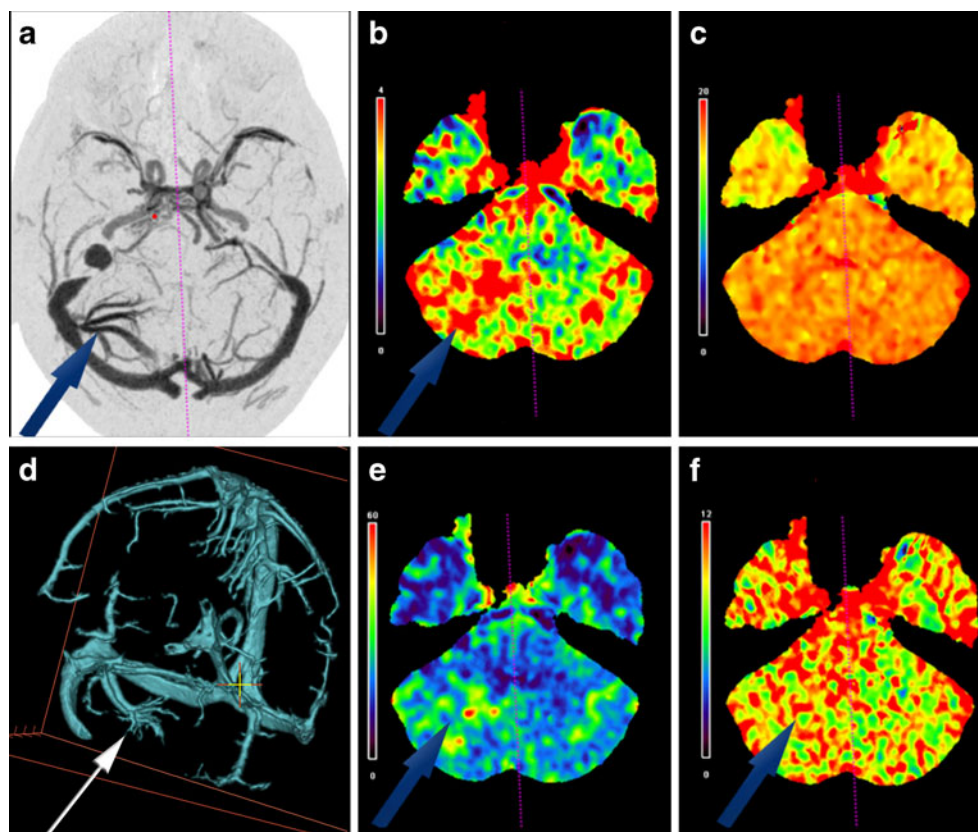
increased venous pressure) [10]. The findings of the present study suggest that anatomical variations in DVA that can influence hemodynamic flow may be characterized by the combination of assessment by CTA-V (Fig. 4d), whole-brain dynamic volume CTP, and 4D DSA.

As reviewed by Hammoud et al. [13], nonhemorrhagic ischemia associated with DVA is uncommon and rarely reported in the literature. A review by Hon et al. [23] of 15 studies that included 714 patients with DVA found that less than 1% were associated with infarction on the initial presentation. The etiology of nonhemorrhagic infarcts associated with DVA has been proposed as thrombosis of the collecting or draining vein [13] and has been identified on angiography [24]. Stenosis at the dural opening of DVA is also frequently noted and this has been proposed as a mechanism for initiating a DVA thrombosis [4, 25]. In this study, no case had clinically discernible stenosis, but case 3 had multiple terminal draining veins that lead into a small dural opening (Fig. 4a, d). DVA that demonstrate thrombotic complications are treated the same as cortical venous or venous sinus thromboses. An identical laboratory workup is required and consideration for treatment with anticoagulation is appropriate. Investigation of procoagulating factors or prothrombotic conditions is also important [10]. Regardless of the treatment method implemented, it is important that the integrity of the DVA be preserved to avoid the substantial neurologic complications previously

documented when it is excised either inadvertently or due to clinical necessity [10, 13, 26]. DVA-associated hemorrhagic and nonhemorrhagic infarctions are rare, but implementation of prevention measures upon identification, such as hydration in warm climates, smoking cessation, or anticoagulant medications for individuals at increased risk of thrombosis as indicated may reduce risk of adverse events.

Although DVA complications are rare, the complications of DVA are more frequently hemorrhagic than ischemic in nature [25, 27, 28]. The Hon et al. [23] review found that 6% with DVA presented with symptomatic hemorrhage and the hemorrhage rate following the first event was 0-1.28% per year for 422 of these 714 patients. In a prospective study by the same authors on 93 adults, one patient presented with symptomatic hemorrhage and there were no symptomatic hemorrhages following the first presentation for a total of 492 person-years of follow-up [23]. Formation of a thrombus within a DVA has also been proposed as a cause of DVA-associated hemorrhage secondary to increased venous pressure [27]. Additionally, DVA hemorrhages may not result from the DVA itself but may be associated with co-occurring or developing anomalies including CM, capillary telangiectasias, and AVMs. Hemorrhage of DVA with an associated CM has been well-documented [1, 7, 9, 16, 29, 30] and Hong et al. [14] described angioarchitectural factors of DVA that may cause

Fig. 5 A 50-year-old female who presented with numbness on the right side of her face (case 1); a juxtacortical left frontal lobe DVA was identified. **a** Upper left axial image is a DSA image collected with slice thickness of 30 mm and then clockwise from left to right axial perfusion images are colorimetric representations of **b** regional CBV, **c** TTP, **d** regional CBF, **e** MTT, and **f** delay
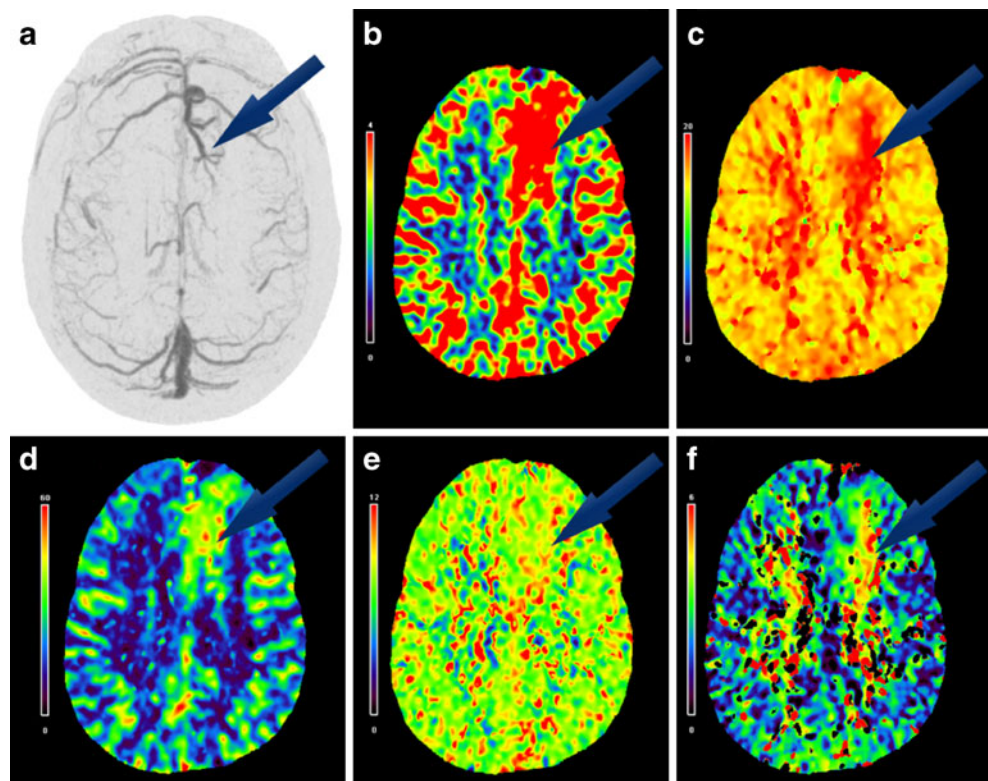
concurrent sporadic CM to form. Further evaluation is required to determine if DVA progression to capillary telangiectasias and CMs or AVM proximity to DVAs can be longitudinally monitored with CTP.

Previous CT technology has not allowed whole-brain visualization and as demonstrated in this study, comprehensive DVA analysis requires whole-brain CTP for visualization of the peripheral or superior cerebral cortices (case 1 in Fig. 5; cases 2, 4, and 5) or in the posterior fossa (case 3 in Fig. 4).

With the recent scientific advances in understanding of the pathophysiology [10] and angioarchitectural factors [14] of DVA coupled with the increasing clinical availability of whole-brain CTP, this preliminary study data indicates that the incremental diagnostic information for DVA can be provided by whole-brain CTP studies. Further investigations are required to use CTP as a method for identifying individuals at greatest risk for adverse clinical outcomes related to DVA. Additionally, it is possible that assessment of the CTP parameters associated with DVA may help to avoid incorrect diagnoses such as arterial infarcts, focal hemorrhage, demyelinating disease [31], neoplasm, or similar appearing abnormalities on CT [13]. Misdiagnosis of DVA and DVA-associated infarcts has been documented and may be secondary to the heterogeneous imaging characteristics of cerebral venous infarctions [32]. Additionally, DVA are frequently not identified on other imaging studies including non-contrast CT and

structural MRI but may be detected with CTP, as was true of case 5 in this study (Table 1).

In order to assess the risk associated with diagnostic procedures, both physical risk and radiation dose must be considered. Due to its interventional nature, conventional angiography has a 0.5% risk of permanent neurologic complication [33] and a typical effective radiation dose of 10.6 mSv [34]. The whole-brain CT imaging protocol used in this study, that included CT DSA and CTP, had an effective dose of 4.3-4.4 mSv (Table 2). Effective radiation dose for 64-slice CTP has been reported as 7.5-11.4 mSv [34]. The whole-brain CTP protocol used in this study is lower than conventional angiography or 64-slice CT and is less than one third of the level reported as acceptable by the FDA for brain perfusion imaging [35]. As with any imaging study, the benefit of the diagnostic information acquired must always be weighed versus the radiation risk.

There were limitations of this study. CTP value variation using ROIs and placement of the ROIs near vessels or artifacts can adversely impact the clinical interpretation of results. Variation with the 8 mm ROIs was increased for two reasons: (1) a HU densities in the ROI are averaged in the vicinity of each voxel together and (2) when the ROI is placed in areas with vessels, the flow and volumes are significantly higher. CTP values obtained within the area of the DVA and in the contralateral hemisphere have different compositions of parenchymal and vascular components and this variability could not be quantified. Vascular and tissue

differentiation could be improved by pixel-by-pixel CTP value evaluations and this could increase precision in defining the range of CTP values at important DVA structures, such as the terminal vein opening. Additionally, no cases had angiographical confirmation of associated pathologies. Finally, expanded CTP studies with higher numbers of patients using standardized system configurations (e.g., hardware, software, and protocols) with human variables (e.g., estimates of cardiac output and hematocrit) incorporated into the DICOM files may help to facilitate individual CTP analyses, as well as comparisons between individuals.

Most DVA are incidental findings on imaging studies and little is known about which individuals will progress to hemorrhagic or ischemic complications. The cases presented suggest that the physiologic appearance of DVA on CT DSA and whole-brain CTP can provide incremental clinical information to practitioners for diagnostic purposes and with future research may help to provide some of the monitoring and prognostic data required to identify the rare subset of patients with DVA that are at increased risk of adverse outcomes.

References

1. Abe T, Singer RJ, Marks MP, Norbash AM, Crowley RS, Steinberg GK (1998) Coexistence of occult vascular malformations and developmental venous anomalies in the central nervous system: MR evaluation. AJNR Am J Neuroradiol 19:51–57
2. Valavanis A, Wellauer J, Yasargil MG (1983) The radiological diagnosis of cerebral venous angioma: cerebral angiography and computed tomography. Neuroradiology 24:193–199
3. Lasjaunias P, Burrows P, Planet C (1986) Developmental venous anomalies (DVA): the so-called venous angioma. Neurosurg Rev 9:233–242
4. Truwit CL (1992) Venous angioma of the brain: history, significance, and imaging findings. AJR 159:1299–1307
5. Sarwar M, McCormick WF (1978) Intracerebral venous angioma. Case report and review. Arch Neurol 35:323–325
6. Garner TB, Del Curling O Jr, Kelly DL Jr, Lancer DW (1991) The natural history of intracranial venous angiomas. J Neurosurg 75:715–722
7. Topper R, Jurgens E, Reul J, Thron A (1999) Clinical significance of intracranial developmental venous anomalies. J Neurol Neurosurg Psychiatry 67:234–238
8. Abla A, Wait SD, Uschold T, Lekovic GP, Spetzler RF (2008) Developmental venous anomaly, cavernous malformation, and capillary telangiectasia: spectrum of a single disease. Acta Neurochir (Wien) 150:487–489
9. Oran I, Kiroglu Y, Yurt A, Ozer FD, Acar F, Dalbasti T, Yagci B, Sirikci A, Calli C (2009) Developmental venous anomaly (DVA) with arterial component: a rare cause of intracranial haemorrhage. Neuroradiology 51:25–32
10. Pereira VM, Geibprasert S, Krings T, Aurboonyawat T, Ozanne A, Toulgoat F, Pongpech S, Lasjaunias PL (2008) Pathomechanisms of symptomatic developmental venous anomalies. Stroke 39:3201–3215
11. McLaughlin MR, Kondziolka D, Flickinger JC, Lunsford S, Lunsford LD (1998) The prospective natural history of cerebral venous malformations. Neurosurgery 43:195–200
12. Camacho DLA, Smith JK, Grimme JD, Keyserling HF, Castillo M (2004) Atypical MR imaging perfusion in developmental venous anomalies. AJNR Am J Neuroradiol 25:1549–1552
13. Hammoud D, Beauchamp N, Wityk R, Yousem D (2002) Ischemic complication of a cerebral developmental venous anomaly: case report and review of the literature. J Comput Tomogr 26:633–636
14. Hong YJ, Chung TS, Suh SH, Park CH, Tomar G, Seo KD, Kim KS, Park IK (2010) The angioarchitectural factors of the cerebral developmental venous anomaly; can they be the causes of concurrent sporadic cavernous malformation? Neuroradiology. doi:10.1007/s00234-009-0640-6
15. Kroll H, Soares BP, Saloner D, Dillon WP, Wintermark M (2009) Perfusion-CT of developmental venous anomalies: typical and atypical hemodynamic patterns. J Neuroradiol. doi:10.1016/j.neurad.2009.09.002
16. San Millan Ruiz D, Delavelle J, Yilmaz H, Gailloud P, Piovan E, Bertramello A, Pizzini F, Rufenacht DA (2007) Parenchymal abnormalities associated with developmental venous anomalies. Neuroradiology 49:987–995
17. Moritake K, Handa H, Mori K, Ishikawa M, Morimoto M, Takebe Y (1980) Venous angiomas of the brain. Surg Neurol 14:95–105
18. Bongartz G, Golding SJ, Jurik AG, Leonardi M, vanMeerten E, Rodríguez R, Schneider K, Calzado A, Geleijns J, Jessen KA, Panzer W, Shrimpton PC, Tosi G (2004) European Guidelines for Multislice Computed Tomography. European Commission. http://w3.tue.nl/fileadmin/sbd/Documenten/Leergang/BSM/European_Guidelines_Quality_Criteria_Computed_Tomography_Eur_16252.pdf. Accessed 9 April 2010
19. Lee C, Pennington MA, Kenney CM (1996) MR evaluation of developmental venous anomalies: medullary venous anatomy of venous angiomas. AJNR Am J Neuroradiol 17:61–70
20. Barnett V, Lewis T (1994) Outliers in statistical data. Wiley, New York
21. Uchida K, Tamura K, Takayama H, Kodaki K, Kawase T, Shiga H, Toya S (1989) Xenon-enhanced CT CBF measurements in intracranial vascular malformations. No Shinkei Geka 17:239–246
22. Matsuda H, Terada T, Katoh M, Ishida S, Onuma T, Nakano H, Yagishita A (1994) Brain perfusion SPECT in a patient with a subtle venous angioma. Clin Nucl Med 19:785–788
23. Hon JM, Bhattacharya JJ, Counsell CE, Papanastassiou V, Ritchie V, Roberts RC, Sellar RJ, Warlow CP, Al-Shahi Salman R (2009) The presentation and clinical course of intracranial developmental venous anomalies in adults: a systematic review and prospective, population-based study. Stroke 40:1980–1985

24. Konan AV, Raymond J, Bourgouin P, Lesage J, Milot G, Roy D (1999) Cerebellar infarct caused by spontaneous thrombosis of a developmental venous anomaly of the posterior fossa. AJNR Am J Neuroradiol 20:256–258

25. Biller J, Toffol GJ, Shea JF, Fine M, Azar-Kia B (1985) Cerebellar venous angiomas. A continuing controversy. Arch Neurol 42:367–370

26. Abe M, Hagihara N, Tabuchi K, Uchino A, Miyasaka Y (2003) Histologically classified venous angiomas of the brain: a controversy. Neurol Med Chir 43:1–10

27. Field LR, Russell EJ (1995) Spontaneous hemorrhage from a cerebral venous malformation related to thrombosis of the central draining vein: demonstration with angiography and serial MR. AJNR Am J Neuroradiol 16:1885–1888

28. Uchino A, Hasuo K, Matsumoto S, Fujii K, Fukui M, Horino K, Tsukamoto Y, Masuda K (1996) Cerebral venous angiomas associated with hemorrhagic lesions. Their MRI manifestations. Clin Imaging 20:157–163

29. Huber G, Henkes H, Hermes M, Felber S, Terstegge K, Piepgras U (1996) Regional association of developmental venous anomalies with angiographically occult vascular malformations. Eur Radiol 6:30–37

30. Wilms G, Bleus E, Demaerel P, Marchal G, Plets C, Goffin J, Baert AL (1994) Simultaneous occurrence of developmental venous anomalies and cavernous angiomas. AJNR Am J Neuroradiol 15:1247–1254

31. Sadeh M, Shacked I, Rappaport ZH, Tadmor R (1982) Surgical extirpation of a venous angioma of the medulla oblongata simulating multiple sclerosis. Surg Neurol 17:334–337

32. Bakac G, Wardlaw JM (1997) Problems in the diagnosis of intracranial venous infarction. Neuroradiology 39:566–570

33. Willinsky RA, Taylor SM, TerBrugge K, Farb RI, Tomlinson G, Montanera W (2003) Neurologic complications of cerebral angiography: prospective analysis of 2, 899 procedures and review of the literature. Radiology 227:522–528

34. Cohnen M, Wittsack HJ, Assadi S, Muskalla K, Ringelstein A, Poll LW, Saleh A, Mödder U (2006) Radiation exposure of patients in comprehensive computed tomography of the head in acute stroke. AJNR Am J Neuroradiol 27:1741–1745

35. Safety Investigation of CT Brain Perfusion Scans: Initial Notification. US Food and Drug Administration (FDA) Center for Devices and Radiologic Health (2009) http://www.fda.gov/MedicalDevices/Safety/AlertsandNotices/ucm185898.htm. Accessed 21 October 2009